Effect of coordination environment of Cu in Cu_2O on the electroreduction CO_2 to ethylene

Yahui Wu,[a,b] Chunjun Chen,[a,b]* Xupeng Yan,[a,b] Shoujie Liu,[e]* Mengen Chu,[d] Haihong Wu,[d]* Jun Ma,[a] Buxing Han[a,b,c,d]*

[a]Beijing National Laboratory for Molecular Sciences, Key Laboratory of Colloid and Interface and Thermodynamics, Institute of Chemistry, Chinese Academy of Sciences, Beijing 100190, P. R. China

[b]School of Chemistry and Chemical Engineering, University of Chinese Academy of Sciences, Beijing 100049, P. R. China

[c]Physical Science Laboratory, Huairou National Comprehensive Science Center, No. 5 Yanqi East Second Street, Beijing 101400, China

[d]Shanghai Key Laboratory of Green Chemistry and Chemical Processes, School of Chemistry and Molecular Engineering, East China Normal University, Shanghai 200062, China

[e] Chemistry and Chemical Engineering of Guangdong Laboratory, Shantou 515063, China.

Experimental Section

Materials: Sodium hydroxide (NaOH), ethanol, acetic acid (purity>99.5%) and acetone were bought from Sinopharm Chem. Reagent Co. Ltd. Cesium hydrogencarbonate ($CsHCO_3$) and copper chloride ($CuCl_2$) were obtained from Alfa Aesar China Co., Ltd. Polyvinylpyrrolidone (PVP, MW=30 000) and L-Ascorbic acid ($C_6H_8O_6$) were purchased from Innochem China Co. Nafion N-117 membrane (0.180 mm thick, ⩾0.90meg g^{-1} exchange capacity) and Nafion D-521 dispersion (5% w/w in water and 1-propanol, ⩾0.92 megg^{-1} exchange capacity) were provided by Alfa Aesar China Co., Ltd. All the chemicals were analytical grade reagents. CO_2 (99.999%) and N_2 (99.999%) were obtained from Beijing Analytical Instrument Company. All of the chemicals were used without further purification.

Synthetic procedures for C-200: The Cu_2O was prepared by wet chemical method.[S1]In a typical experiment, 0.5 mmol $CuCl_2$ was dissolved in 50 mL deionized water by stirring at 55℃. Then, 5 mL NaOH solution (2 mol/L) was added dropwise with adequately stirring for 0.5 h. 5.0 mL ascorbic acid aqueous solution (0.6 mol/L) was added into the solution, keep stirring for 5 h. The resulting precipitate was collected by centrifugation and decanting and washed thoroughly with deionized water and ethanol several times. The final product was dried in a vacuum oven at 60℃ over night. The C-200 was obtained.

Synthetic procedures for C-500, O-500: C-500 and O-500 were synthesized by by similar way as preparing C-200. Typically, 60 mL NaOH solution (2 mol/L) was added dropwise into 600 mL $CuCl_2$ (0.01 mol/L) which containing a certain amount of polyvinylpyrrolidone (PVP MW=30000) (cube: 0 g; octahedral: 53.28 g), and the solution was adequately stirred for 0.5 h at 55℃, and then 60 mL ascorbic acid aqueous solution (0.6 mol/L) added into the solution, keep stirring for 5 h. The resulting precipitate was collected by centrifugation and decanting and washed thoroughly with deionized water and ethanol several times. The final product was dried in a vacuum oven at 60℃ overnight.

Synthetic procedures for O-45, O-90 and O-135: We take preparation of O-45 as the example to discuss the procedure. 0.1g O-500 was dispersed into 200 mL acetic acid (PH=3).The mixture was stirred for 45 min with a magnetic stirrer at 400 rpm at 30℃. Then, the resulting precipitate was

collected by centrifugation and decanting and washed thoroughly with deionized water and ethanol several times. The final product was dried in a vacuum oven at 60℃ overnight and O-45 was obtained. The procedures for preparing O-90 and O-135 were similar, and the main difference was that the stirring were 90 min and 135 min, respectively.

Semi-in-situ X-ray photoelectron spectroscopy: In order to detect the valence of Cu during the reaction, the catalyst samples for XPS characterization were prepared in the glove box. In the experiments, the electrolysis was carried out for 20 min with a typical H-type cell using N_2 or CO_2-saturated 0.1 M $CsHCO_3$ electrolyte. Subsequently, the electrode plate was washed with water and acetone and transferred to the glove box. The obtained electrode plate was cut into 3 × 3 mm and glued on a stage. The stage could be evacuated into vacuum to prevent the samples to be oxidized by the air. The subsequent testing processes were the same as the common X-ray photoelectron spectroscopy.

The operando X-ray adsorption spectroscopy: The operando X-ray adsorption spectroscopy (XAS) measurements were performed using a modified H-cell (the experimental equipment was shown in Figure S5) at the 1W1B, 1W2B beamline at Beijing Synchrotron Radiation Facility (BSRF).

Electrode preparation and pretreatment: 5 mg sample and 15 uL 5% Nafion D-521 were dispersed in 1 mL acetone to form homogeneous solution with the help of ultrasound. Then,10 uL dispersion was spread onto the glassy carbon electrode (r=3 mm), which was pretreated by electroreduction in 0.1 mol / L $CsHCO_3$ for 20 min at -1.9 V vs. RHE.

Electrochemical study: All the electrochemical experiments were carried out on the electrochemical workstation (CHI 660E, Shanghai CH Instruments Co., China). Linear sweep voltammetry (LSV) scans were conducted in a single compartment cell with a three electrodes configuration, which consisted of a platinum gauze as counter electrode, working electrode, and Ag/AgCl as reference electrode. Prior to experiment, the electrolyte was bubbled with CO_2 or N_2 at least 30 min to form CO_2 or N_2 saturated solution. LSV measurement in the gas-saturated electrolytes was conducted in the potential range of 0 V to -1.9 V versus RHE at sweep rate of 20 mV s^{-1}.The electrolyte was stirred during the experiment. All potentials cited in this work were referenced to the RHE. (E (vs RHE) = E (vs Ag/AgCl) +0.0591 × pH+ 0.209 V. The pH is 8.2.

Controlled potential electrolysis of CO_2 was conducted at 25 °C in a H-type cell[S2] with a counter

anode (platinum gauze), working cathode, and an Ag/AgCl reference electrode. In the experiment, Nafion 117 proton exchange membrane was used to separate the anode and cathode compartments. $CsHCO_3$ aqueous solution (0.1 M) were used as electrolyte. It is worthy note that electrode solution for each reaction is 30 mL and CO_2 was bubbled with the electrolyte for 30 min before electrolysis, keep stirring and the electrolysis was carried out with CO_2 bubbling (20 mL/min).

Calculation of current density: In this work, the current density was obtained by dividing the current by the geometric area of electrode. The geometric area of electrode was 0.2826 cm^{-2}.

Product analysis: Liquid products are detected by ^1H NMR (Bruker AV II 400 HD spectrometer) in D_2O with phenol as an internal standard. CO_2 electroreduction gaseous products were collected through air bags and further analyzed by gas chromatography (GC, Agilent 7890B) which was equipped with FID and TCD detectors. The FE was calculated according to the following equations.

liquid products:

$$FE = \frac{moles\ of\ \ products}{Q / nF} \times 100\ \%$$

(Q: electric quantity of the electrochemical reaction; F: Faraday constant; n: number of electrons)

Gasous products:

$$FE = \frac{moles\ of\ \ products}{Q / nF} \times 100\ \%$$

(Q: electric quantity of the electrochemical reaction; F:Faraday constant;n: number of electrons)

Electrochemical impedance spectroscopy (EIS) study: The EIS measurement was carried out in $CsHCO_3$ aqueous solution (0.1 M) at an open circuit potential (OCP) within the frequency range of 10^{-2} to 10^5 Hz Hz and at a amplitude of 5 mV.

Double-layer capacitance (C_{dl}) measurements: The C_{dl} value is proportional to electrochemical active surface area. The C_{dl} value was estimated based on the scan rate dependence of cyclic voltammetry (CV) to measure the capacitance current associated with the double layer. The CV ranged from -0.05 V to -0.15 V vs. RHE. The C_{dl} was estimated by plotting Δj (j_a-j_c) at -0.1 V against the scan rates (j_a = anodic current density, j_c=cathodic current density), the slope was twice that of C_{dl}. The scan rates were 20, 30, 50, 80, 100 and 120 mV s^{-1}.

The ECSAs of the working electrodes was calculated according to equation ECSAs = RfS, where S is the real surface area of the working electrode and Rf was the roughness factor of the working electrode. Notably, S was generally equal to the geometric area of working electrode (in this work, S = 0.2826 cm^{-2}). The roughness factor (Rf) can be calculated from the equation Rf = Cdl/a. The Cdl is double-layer capacitance for the working electrode and a is double-layer capacitance for the corresponding smooth metal electrode. The roughness factor of O-500 was defined to be 1, then the normalized current density can be calculated according to roughness factor of different catalysts.

Product analysis. The gaseous product of electrochemical experiments was collected using a gas bag and analyzed by gas chromatography (GC, HP 4890D), which was equipped with TCD detectors using argon as the carrier gas. The liquid product was analyzed by ^{1}H NMR (Bruker Avance III 400 HD spectrometer) in Deuterium for dimethyl sulfoxide.

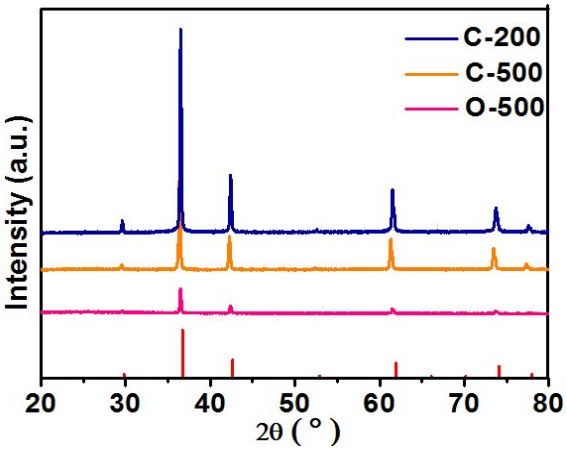

Figure S1. XRD patterns of different Cu_2O samples.

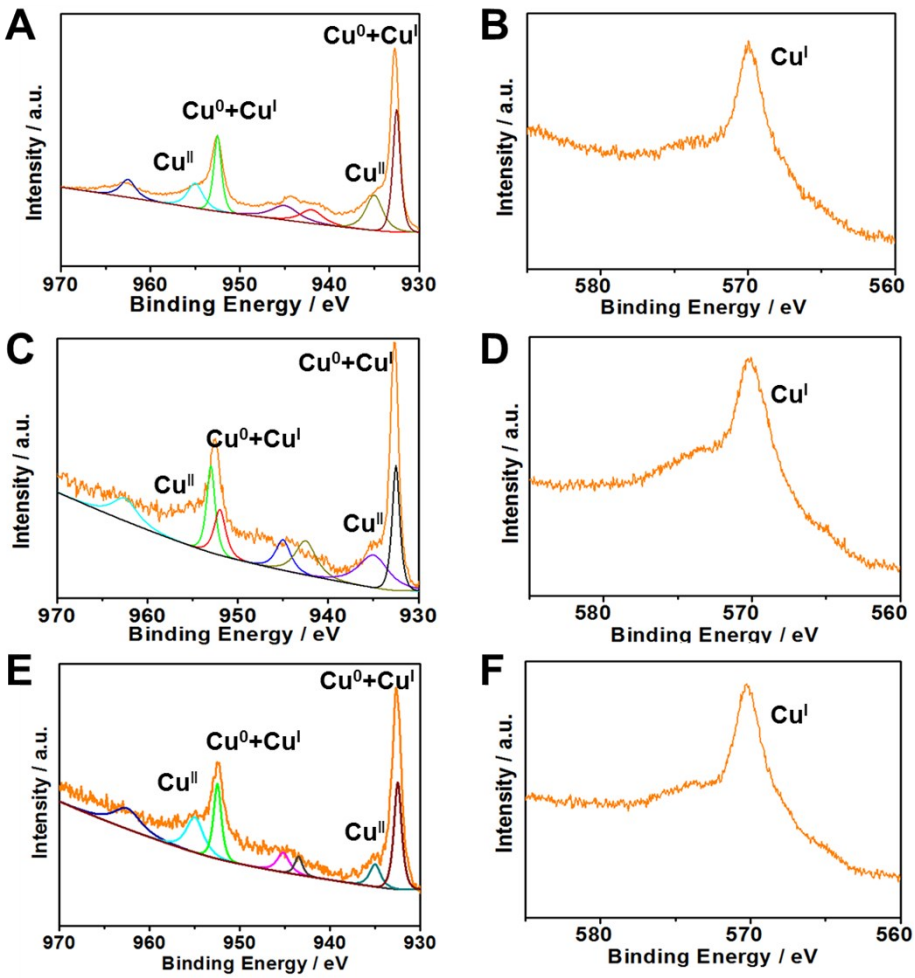

Figure S2. XPS spectra of Cu 2p orbits and LMM Auger spectra of C-200 (A, B); XPS spectra of Cu 2p orbits and LMM Auger spectra of C-500 (C, D); XPS spectra of Cu 2p orbits and LMM Auger spectra of O-500 (E, F).

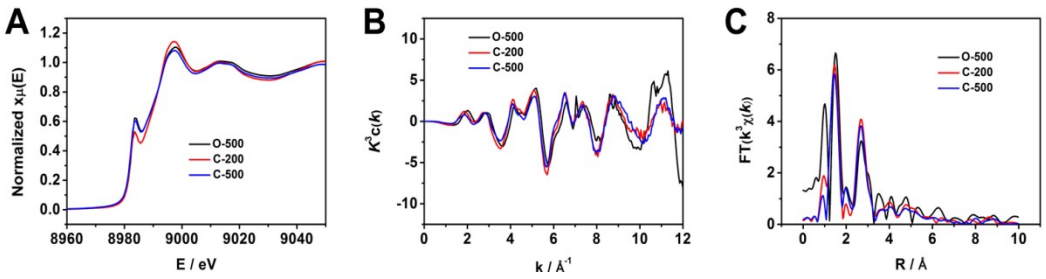

Figure S3. XANES spectra at the Cu K-edge for different Cu_2O catalysts(A); Cu K-edge extended XAFS oscillation function $k^3w(k)$ (B); The corresponding Fourier transforms $FT(k^3w(k))$ (C).

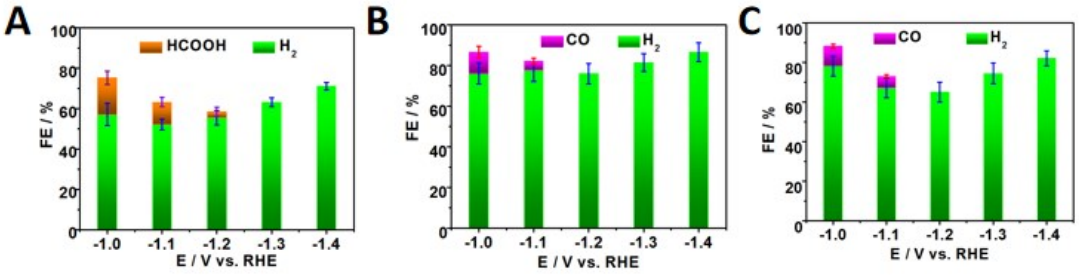

Figure S4. Faradaic efficiency of other products over C-200 (A), C-500 (B), and O-500 (C).

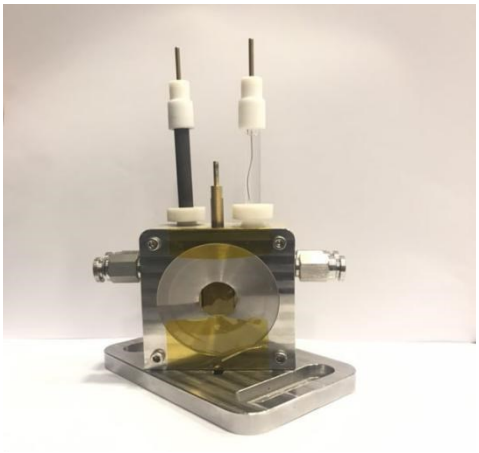

Figure S5. The optical photograph of operando-XAFS device.

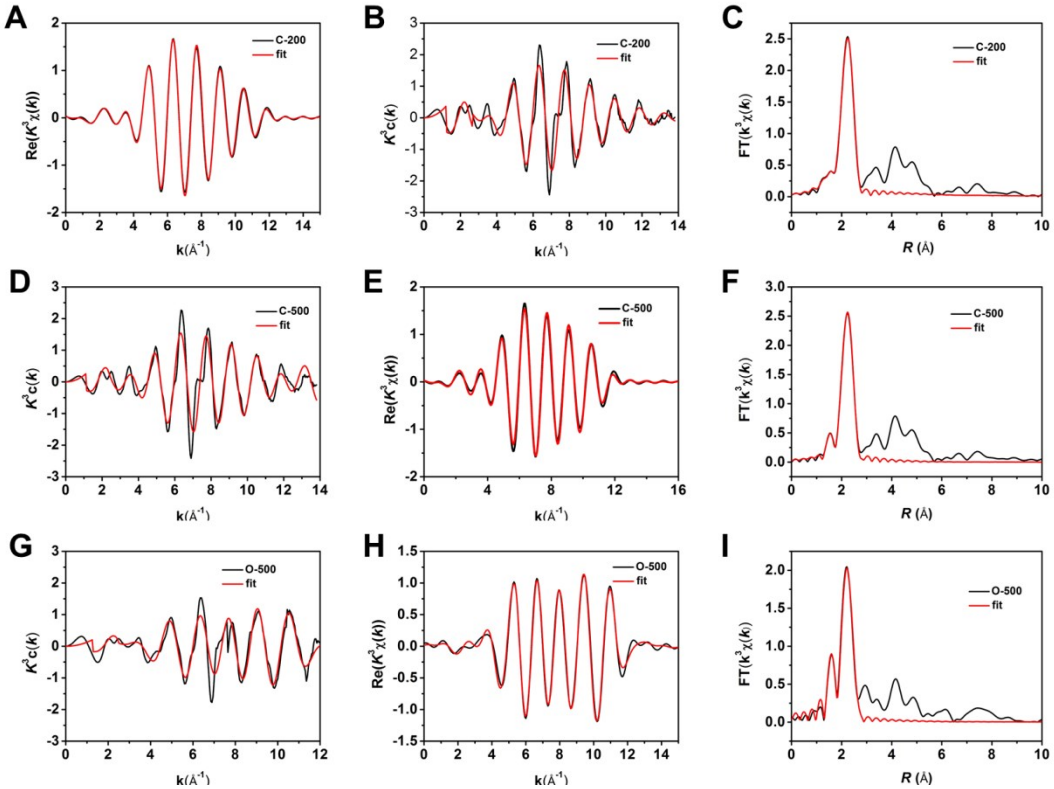

Figure S6. The EXAFS data fitting results of C-200, C-500 and O-500.

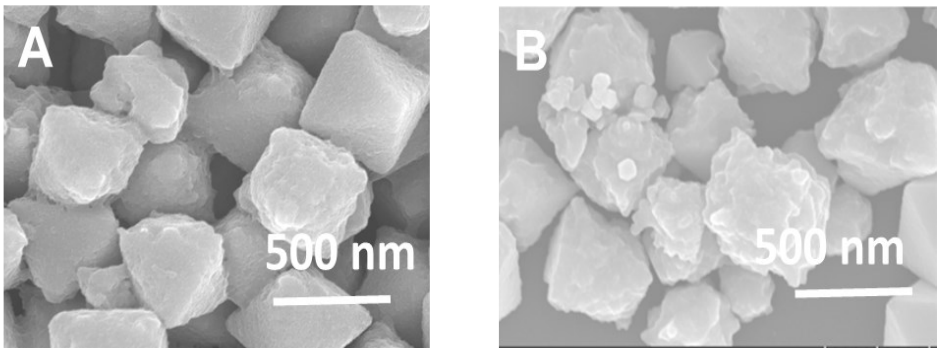

Figure S7. The SEM image of O-500-45 (A); The SEM image of O-500-135 (B).

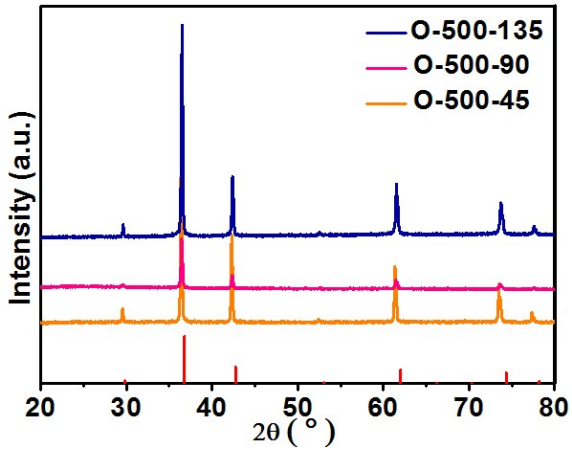

Figure S8. XRD patterns of different Cu_2O samples.

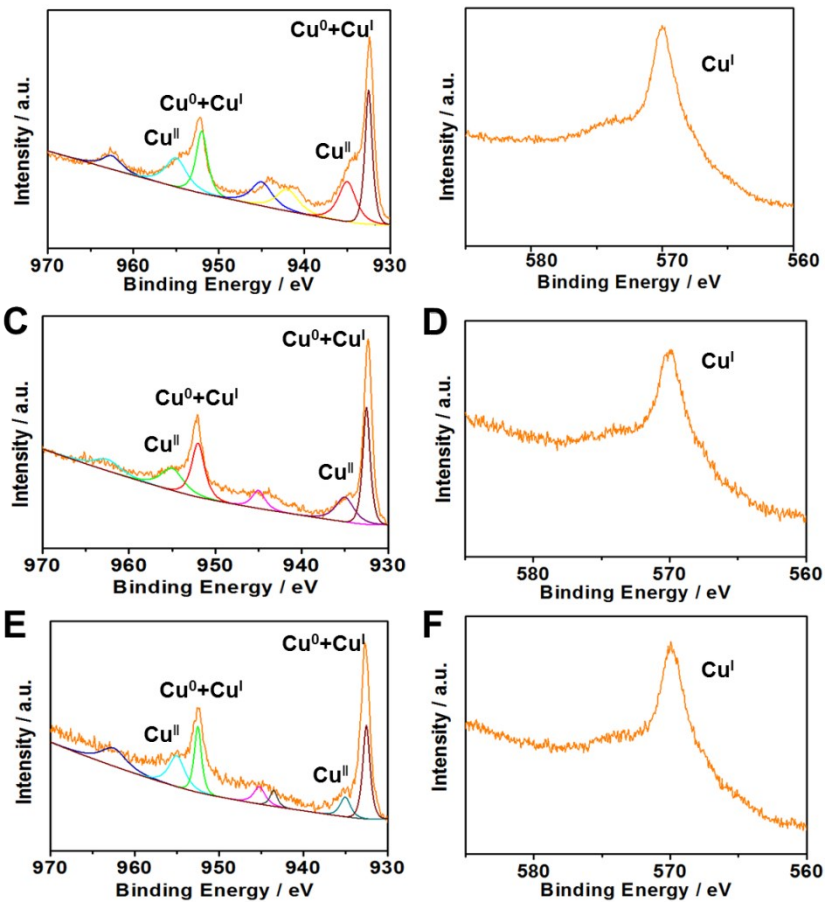

Figure S9. XPS spectra of Cu 2p orbits and LMM Auger spectra of O-500-45 (A, B); XPS spectra of Cu 2p orbits and LMM Auger spectra of O-500-90 (C, D); XPS spectra of Cu 2p orbits and LMM Auger spectra of O-500-135 (E, F).

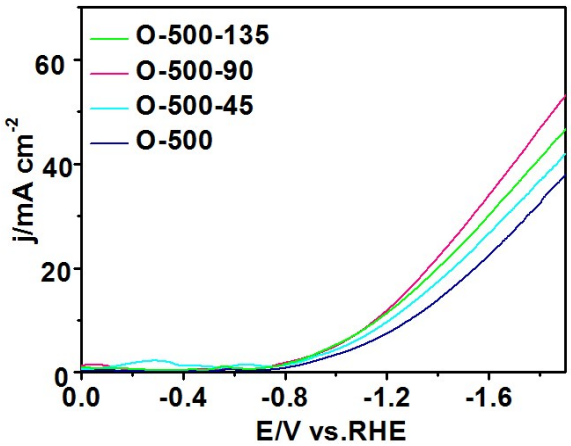

Figure S10. LSV curves on different electrodes with a scan speed of 20 mV s^{-1} in CO_2-saturated 0.1 M $CsHCO_3$ electrolyte.

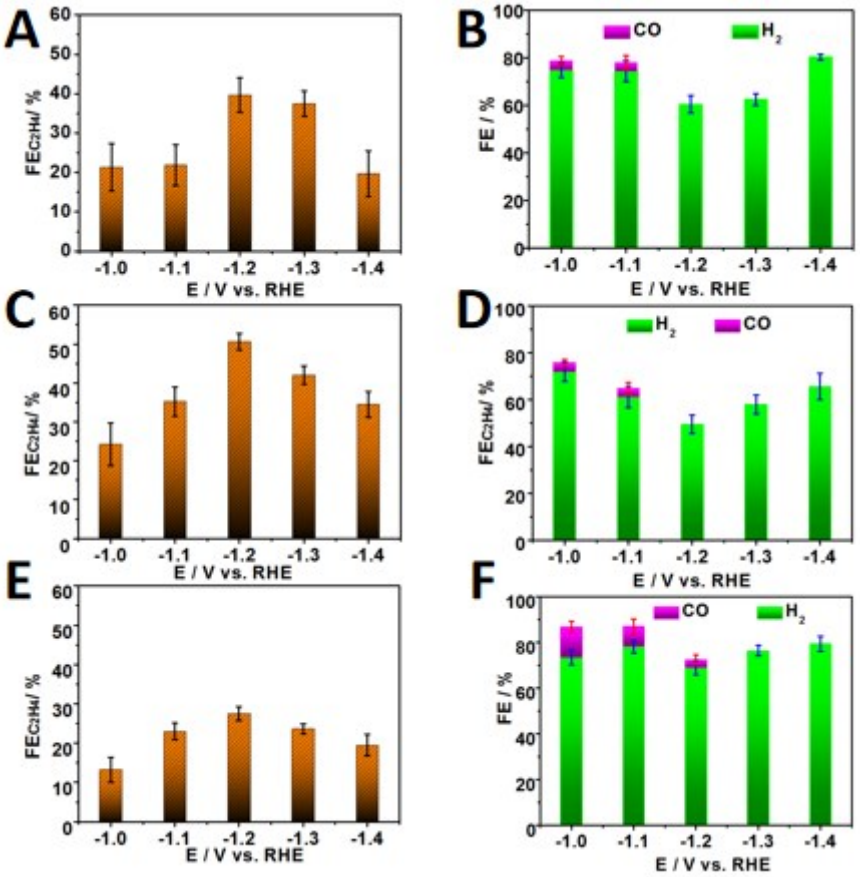

Figure S11. The Faradaic efficiency of C_2H_4 (A) and other products (B) of O-500-45; The Faradaic efficiency of C_2H_4 (C) and other products (D) of O-500-90; The Faradaic efficiency of C_2H_4 (E) and other products (F) of O-500-135.

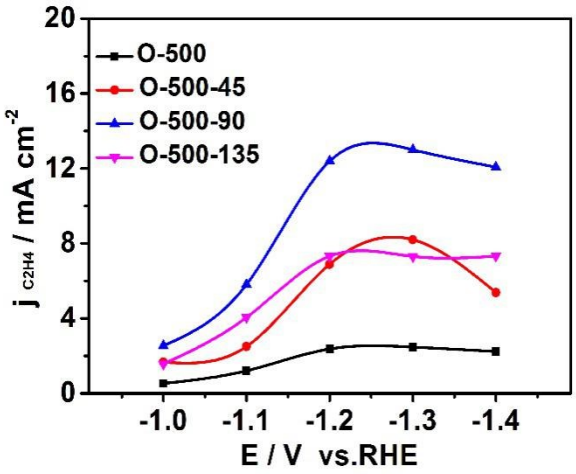

Figure S12. The partial current density of C_2H_4 over different Cu_2O catalysts (O-500, O-500-45, O-500-90 and O-500-135) .

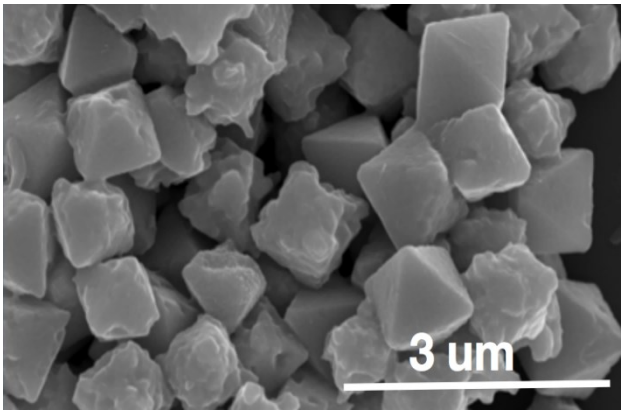

Figure S13. SEM images of O-500-90 catalyst after reaction.

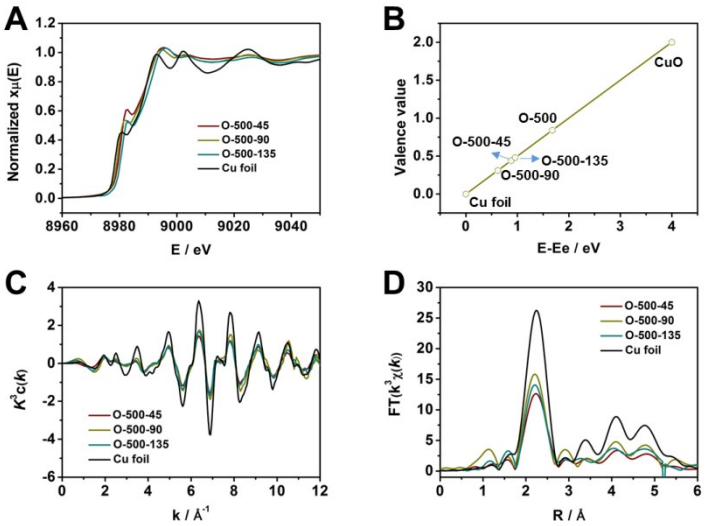

Figure S14. XANES spectra at the Cu K-edge for different Cu_2O catalysts at -1.2V vs. RHE (A); The apparent valence states from the XANES (B); Cu K-edge extended XAFS oscillation function $k^3w(k)$ (C); The corresponding Fourier transforms $FT(k^3w(k))$ (D).

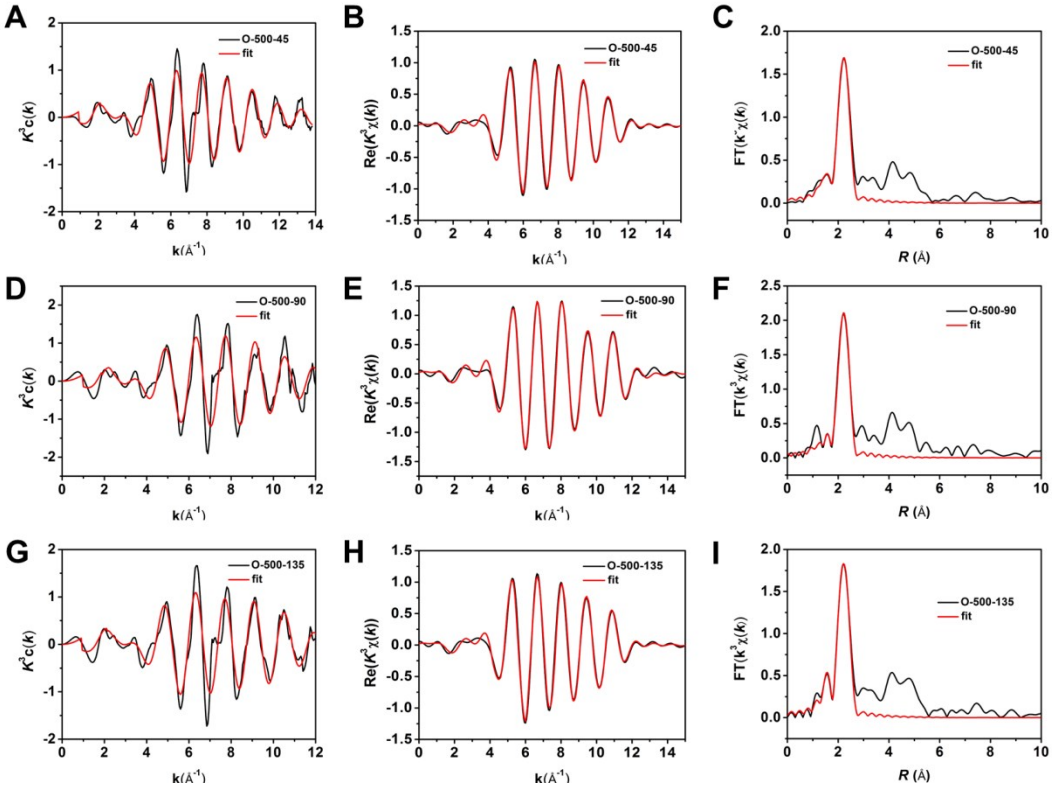

Figure S15. The EXAFS data fitting results of O-500-45, O-500-90 and O-500-135.

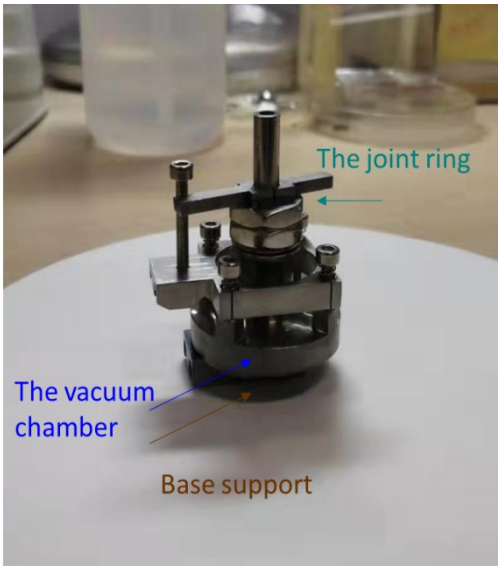

Figure S16. The optical picture of the semi-in-situ XPS cell. The obtained electrode plate was cut into 3 × 3 mm and glued on the support. The vacuum chamber could be evacuated into vacuum to prevent the samples to be oxidized by the air.

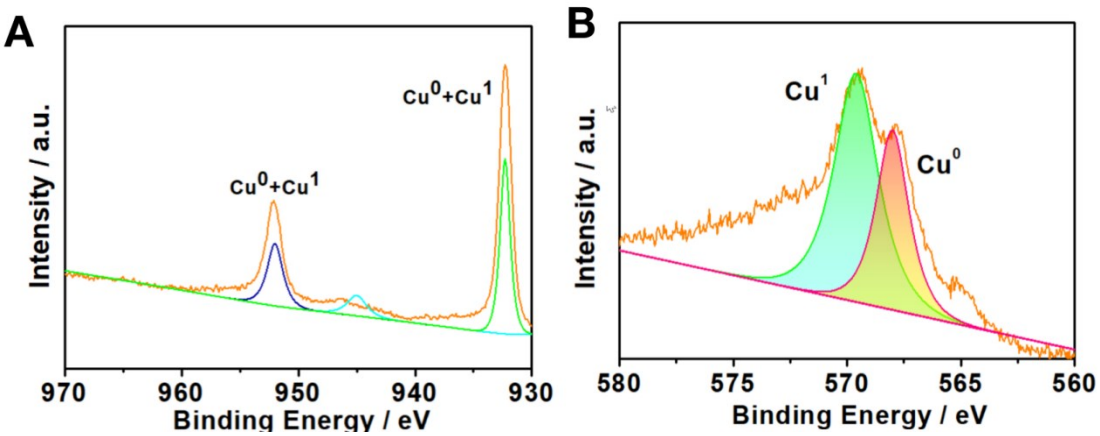

Figure S17. Semi-in-situ-XPS spectra of Cu 2p orbits and LMM Auger spectra of O-500-45 (A, B) in CO2-saturated 0.1 M $CsHCO_3$ electrolyte at -1.2 vs. RHE.

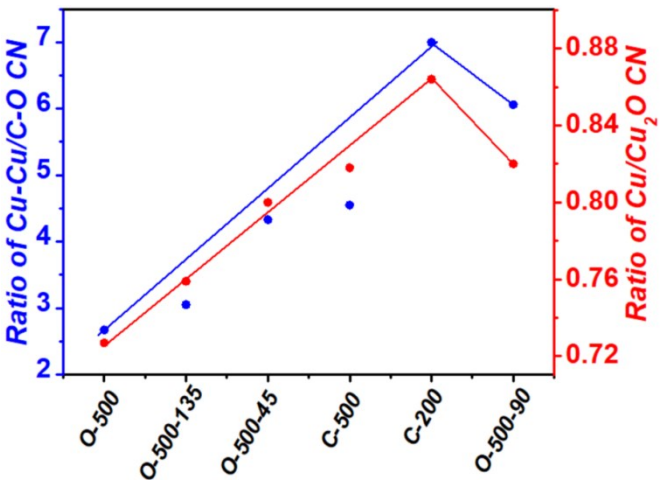

Figure S18. The ratio of Cu/Cu_2O and Cu-Cu /Cu-O CN for different catalysts.

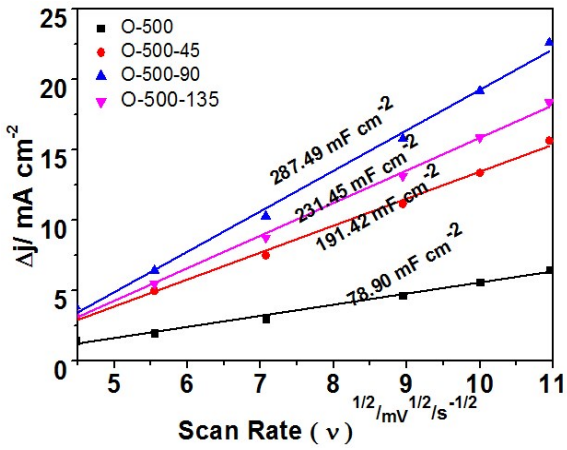

Figure S19. Charging current density differences plotted against scan rates of the different Cu_2O catalysts.

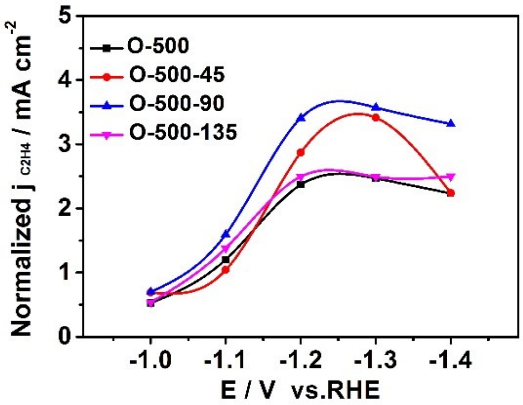

Figure S20. The normalized C_2H_4 partial current density over different Cu_2O catalysts (O-500, O-500-45, O-500-90 and O-500-135) .

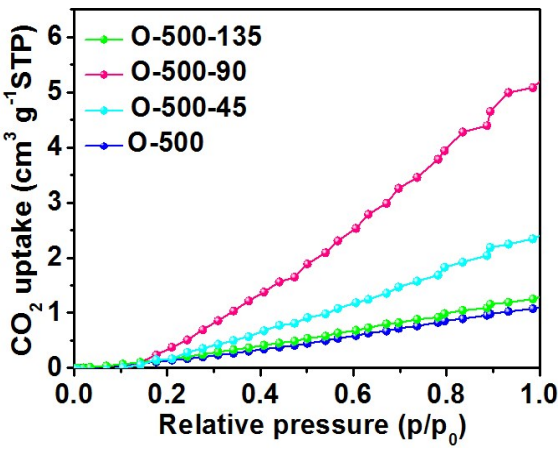

Figure S21. The CO_2 adsorption behaviors for different Cu_2O catalysts.

The adsorption isotherms of CO_2 were determined at 298 K in the pressure range of 0-1 atm on a TriStar II 3020 device.

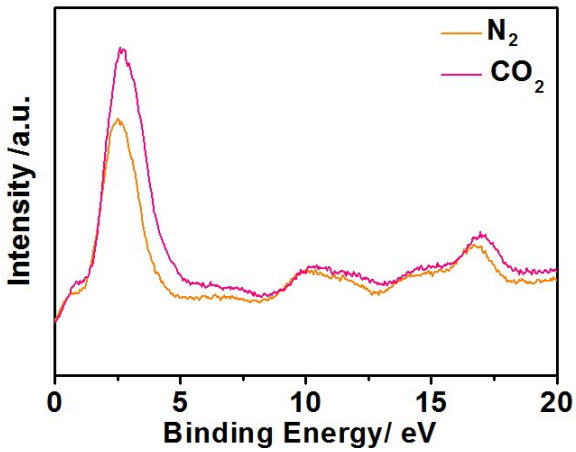

Figure S22. Semi-in-situ-XPS valence band spectra of O-500-90 in N_2-saturated 0.1 M $CsHCO_3$ electrolyte and CO_2-saturated 0.1 M $CsHCO_3$ electrolyte at -1.2 vs. RHE.

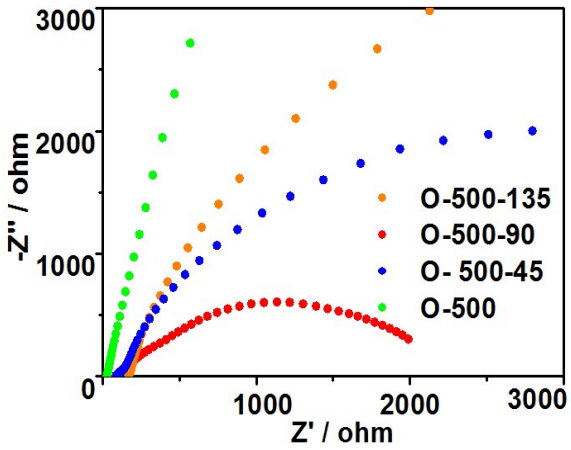

Figure S23. Nyquist plots for different electrodes in CO_2-saturated 0.1 M $CsHCO_3$ electrolyte.

Table S1. Structural parameters of different Cu_2O catalysts extracted from the EXAFS fitting. (S_0^2=0.85)

Sample	Scattering pair	CN	R(Å)	$\sigma^2(10^{-3}Å^2)$	ΔE_0(eV)
O-500	Cu-O	3.0±0.8	1.90±0.02	5.4±1.1	-4.9±1.5
	Cu-Cu	8.0±0.9	2.53±0.02	6.8±1.8	4.3±1.5
O-500-45	Cu-O	1.2±0.7	1.89±0.02	5.4±0.9	-4.9±1.5
	Cu-Cu	5.2±0.6	2.53±0.02	6.8±0.9	4.3±1.5
O-500-90	Cu-O	1.2±0.8	1.90±0.02	5.4±1.3	-4.9±1.5
	Cu-Cu	8.1±0.5	2.53±0.02	6.9±1.6	4.3±1.5
O-500-135	Cu-O	2.0±0.8	1.90±0.02	5.4±1.7	-4.9±0.8
	Cu-Cu	6.1±0.5	2.53±0.02	6.8±1.2	4.3±1.5
C-200	Cu-O	1.3±0.8	1.90±0.02	5.4±1.4	-4.9±1.5
	Cu-Cu	9.1±0.9	2.53±0.02	6.8±0.8	4.3±1.5
C-500	Cu-O	2.0±0.8	1.90±0.02	5.4±1.4	-4.9±1.5
	Cu-Cu	9.1±0.9	2.53±0.02	6.9±0.7	4.3±1.5

S_0^2 is the amplitude reduction factor S_0^2=0.85; CN is the coordination number; R is interatomic distance (the bond length between central atoms and surrounding coordination atoms); σ^2 is Debye-Waller factor (a measure of thermal and static disorder in absorber-scatterer distances); ΔE_0 is edge-energy shift (the difference between the zero kinetic energy value of the sample and that of the theoretical model). R factor is used to value the goodness of the fitting.

Table S2. Comparision of the performances of various catalysts for C_2H_4 production .

Samples	electrolyte	E vs. RHE	Current density	FEC_2H_4 (%)	references
O-500-90	0.1 M $CsCO_3$	-1.2	24.5 mA cm^{-2}	50.6	This work
Cu-on-Cu_3N	0.1 M $KHCO_3$	-0.95	25.0 mA cm^{-2}	39.0	S3
Graphite/carbon NPs/Cu/PTEF	10 M KOH	-0.54	275.0 mA cm^{-2}	66.0	S4
Plasma-oxidized Cu	0.1 M $KHCO_3$+ 0.3M KI	-1.0	45.5 mA cm^{-2}	47.6	S5
Cu nanocube	0.1 M KHCO3	-1.0	35.0 mA cm^{-2}	45.0	S6
Cu_2O film	0.1 M $KHCO_3$	-0.99	12.3 mA cm^{-2}	40.3	S7
Cu nanoparticle ensembles	0.1 M $CsHCO_3$	-0.75	10.0 mA cm^{-2}	50.0	S8
electrodeposited Cu_2O	0.1 M $KHCO_3$	-1.1	10.0 mA cm^{-2}	33.0	S9
electrodeposited Cu_2O	0.5 M $KHCO_3$	-1.05	13.6 mA cm^{-2}	26.0	S10
Oxide-derived Cu Foam	0.5 M $NaHCO_3$	-1.0	7.0 mA cm^{-2}	19.0	S11
Oxide-derived Cu	0.1 M $KHCO_3$	-0.95	10.5 mA cm^{-2}	5.0	S12
Oxide-derived Cu Foam	0.5 M $NaHCO_3$	-1.6	3.0 mA cm^{-2}	18.0	S13
Cu_2O NPs	0.5 M $KHCO_3$	-1.1	22.0 mA cm^{-2}	59	S14

References

S1 Q. Hua, D. Shang, W. Zhang, K. Chen, S. Chang, Y. Ma, Z. Jiang, J. Yang, W. Huang, *Langmuir.* **2011**, *27*, 665-671.

S2 C. Chen, X. Sun, L. Lu, D. Yang, J. Ma, Q. Zhu, Q. Qian, B. Han, *Green Chem.* **2018**, *20*, 4579-4583.

S3 Z. Liang, T. Zhuang, A. Seifitokaldani, J. Li, C. Huang, C. Tan, Y. Li, P. D. Luna, C.T. Dinh, Y. Hu, Q. Xiao, P. Hsieh, Y. Wang, F. Li, R. Quintero-Bermudez, Y. Zhou, P. Chen, Y. Pang, S. Lo, L. Chen, H. Tan, Z. Xu, S. Zhao, D. Sinton and E. H. Sargent, *Nat. Commun.* **2018**, *9*, 3828.

S4 C. Dinh, T. Burdyny, M.G. Kibria, A. Seifitokaldani,C. M. Gabardo, F. P. G. Arquer, A. Kiani,J. P. Edwards, P.D. Luna, O.S. Bushuyev, C. Zou,R. Quintero-Bermudez, Y. Pang, D. Sinton, E. H. Sargent, *Science.* **2018**, *360*, 783-787.

S5 D. Gao, F. Scholten, B. R. Cuenya, *ACS Catal*. **2017**, *7*, 5112-5120.

S6 Gao, D. F.; Zegkinoglou, I.; Divins, N. J.; Scholten, F.; Sinev, I.; Grosse, P.; Roldan Cuenya, B. *ACS Nano.* **2017**, *11*, 4825-4831.

S7 Ren, D.; Deng, Y. L.; Handoko, A. D.; Chen, C. S.; Malkhandi, S.; Yeo, B. S. *ACS Catal.* **2015**, *5*, 2814-2821.

S8 Chen, C. S.; Handoko, A. D.; Wan, J. H.; Ma, L.; Ren, D.; Yeo, B. S. *Catal. Sci. Technol.* **2015**, *5*, 161-168.

S9 Kim, D.; Kley, C. S.; Li, Y.; Yang, P. *Acad. Sci*. **2017**, *114*, 10560 – 10565.

S10 Kim, D.; Lee, S.; Ocon, J. D.; Jeong, B.; Lee, J. K.; Lee, *J. Phys. Chem. Chem. Phys.* **2015**, *17*, 824-830.

S11 Dutta, A.; Rahaman, M.; Luedi, N. C.; Mohos, M.; Broekmann, P. *ACS Catal.* **2016**, *6*, 3804-3814.

S12 Li, C. W.; Kanan, M. W. *J. Am. Chem. Soc.* **2012**, *134*, 7231-7234.

S13 Dutta, A.; Rahaman, M.; Luedi, N. C.; Mohos, M.; Broekmann, P. *ACS Catal*. **2016**, *6*, 3804 – 3814.

S14 Y. Gao, Q. Wu, X. Liang, Z. Wang, Z. Zheng, P. Wang, Y. Liu, Y Dai, M. Whangbo and B. Huang, *Adv. Sci.* **2020**, 1902820.